

EMPIRICAL AIRFLOW PATTERN DETERMINATION OF REFRIGERATED BANANA CONTAINERS USING THERMAL FLOW SENSORS

Chanaka Lloyd^{1,2,*}, Safir Issa^{1,2}, Walter Lang¹, Reiner Jedermann¹

¹ *Institute for Microsensors, -actuators and -systems (IMSAS), University of Bremen, Germany.*

² *International Graduate School for Dynamics in Logistics (IGS), University of Bremen, Germany.*

* **Correspondence:** Chanaka Lloyd clloyd@imsas.uni-bremen.de
University of Bremen FB1/MCB, Otto-Hahn-Allee NW1, D-28359 Germany.

Keywords: Airflow, airflow mapping, flow sensor, wireless sensor networks, fruit logistics

Abstract

Inadequate or irregular ventilation in refrigerated containers leads to inhomogeneous temperature distribution in transported foods, which creates hotspots. Hotspots result in loss of food quality and decrease of monetary value of food. Therefore, understanding the behavior of airflow inside refrigerated containers and establishing its relationship to temperature help realize the areas prone to hotspot creation. In order to measure the distributed airflow speed in gaps in containers, a special wireless airflow sensor was designed and produced using a thermal flow sensor. The field trials were carried out in a specially equipped refrigerated container partially filled with bananas, under the Intelligent Container project. The preliminary results presented in this paper show the measurements done in various gaps of the container and how the air flow varies from the reefer side to the door side.

1 Introduction

Food logistics hold prominent importance in EU, especially agri-food within it is accounted to as much as 25% of the international EU transports [1]. In the case of perishable food, losses suffered during transportation are significant in terms of volume and monetary value [2]. The main loss is the deterioration of the food quality and, therefore, high economic losses to the traders and low quality produce to the consumers.

Perishable foods such as vegetables and fruits that are transported over long distances via sea or land require good atmospheric control in order to maintain the foods at the desired temperature. The lack of or inefficient temperature control causes temperature rise and deteriorates the quality of the perishable foods. However, even if the temperature of the containers in which the food is transported is indicated (by the in/out temperature measured at the reefer, i.e. the refrigeration unit) as being maintained, the localized hotspot phenomena cannot be disregarded.

Breathable fruits and vegetables ripen faster if the correct temperature is not maintained. Ventilation within containers over its entire volume is not even and therefore the desired temperature may not be maintained homogeneously. Hotspots are created in such situations where the temperature in isolated localities within a container is increased due to accumulation of heat produced by the fruits, further enhancing the premature ripening process. In this regard, the analysis of air flow—in correlation with temperature—within a container is helpful in understanding where and how such hotspots are created.

The Intelligent Container [3] project, among other objectives, assesses hotspots created within containers, e.g. in containers transporting bananas from Costa Rica to Germany. There have been extensive studies on temperature profiling within containers, but not airflow profiling. This work attempts to understand the airflow distribution within refrigerated containers filled with bananas. This is done by means of measuring the airflow speed at distributed locations in the container. Due to the lack of suitable wireless devices to measure the airflow, a new wireless airflow sensor was designed, manufactured and calibrated. Fifteen airflow sensors were distributed within a partially filled container in order to monitor the airflow speed at different locations.

Section 2 details the custom-made airflow sensor using the IMSAS thermal flow sensor. Section 3 is about the field trials and the types of airflow measurements carried out in the Intelligent Container. The results of the airflow tests are given in Section 4. It also contains analysis of a subset of the measurement data. Section 5, Conclusion and Outlook, summarizes the analysis conclusions and provides a glimpse of the future research path of airflow measurements.

2 Airflow Sensor

The airflow sensor is based on the IMSAS thermal flow sensor [4,8]. The miniature thermal flow sensor (Figure 1(b)) works on the principle of voltage difference between two thermopiles. A heater element in the sensor is powered up and provided with a known amount of power. This power is maintained throughout the measurement period. This method of sampling the sensor is called the Constant Power (CP) method. The heat dissipation profile of the heater element is disturbed when the air passes over the sensor membrane. This change is measurable by the difference of the voltage between the two thermopiles.

The airflow sensor is integrated onto a wireless TelosB platform that is based on IEEE 802.15.4. The sensor has 4 layers: thermal flow sensor, CP circuit, TelosB and battery (Figure 2(bottom)).

2.1 Reading the airflow sensor

The CP circuit schematic is shown in Figure 1(a) and its real circuit is shown in Figure 2(bottom). CP circuit assures that the thermal flow sensor is sampled only when the power of the heater element H is maintained at the desired level (P_{REF} ; for this work $P_{REF} = 5 \text{ mW}$ was used). Higher sensor sensitivity is achieved for higher heater power levels. However, to preserve the battery power of wireless sensor nodes, a low power level was used.

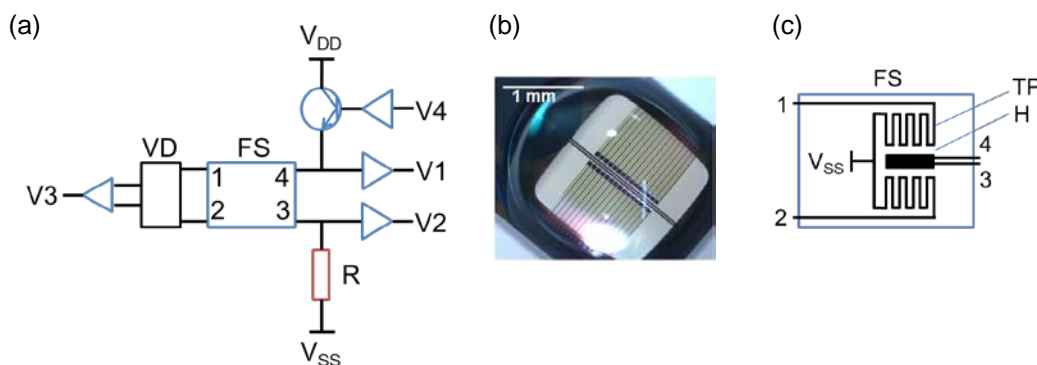


Figure 1: Constant Power (CP) circuit schematic (a); Magnified thermal flow sensor (b); Thermal Flow Sensor (FS) schematic (c).

In Figure 1(a), VD is a high impedance Voltage Divider; FS is the Flow Sensor, further illustrated in Figure 1(c) (representative schematic only); H is the Heater element and TP are the Thermopiles of the thermal flow sensor; V1, V2 are voltage readings at terminals 3 and 4 in Figure 1(c); V3 is the thermopile voltage difference after VD; and, V4 is the DAC-out from TelosB, a control signal based on the control algorithm.

The power (P_H) applied to the heater element H is calculated as the voltage across H (i.e. $V1 - V2$) multiplied by the current through H (i.e. $V2/R$). R is a precision resistor with low variance on temperature change. A control loop, with dynamic proportional feedback, is run in the TelosB to check if P_H is in this range: $(P_{REF} - \Delta P) \leq P_H \leq (P_{REF} + \Delta P)$, where the constant $\Delta P = 0.1 \text{ mW}$. This value is predefined, based on the DAC output and its discrete behavior. The control loop is able to converge on the desired power range within less than a maximum of 80 ms; this is normally when the desired

power level is far off the initial power level when the sensor is powered on. The subsequent convergence steps take less than 10 ms. A complete sensor is shown in Figure 2.

2.2 Calibrated, Field-ready Airflow Sensor

Calibration

The calibration method was based on the comparison between both readings of the airflow sensor and a reference device [5]. The reference device is a calibrated thermo-anemometer (VT200, KIMO Instruments, France). The air flow was controlled by a MFC (Mass Flow Controller) of 1000 SLM (Standard Liters per Minute) and guided into a plexiglas pipe of 62 mm in diameter. At a distance of 1 m from the inlet, through a small opening, the reference device's probe was inserted and sealed. The reference probe and the airflow sensors were placed (not at the same time) in the pipe, where the probe head of the reference device and the air channel on the airflow sensors were carefully aligned with the center line of the test pipe. They were exposed to fifteen successive flow steps of 20 SLM each, with each step lasting 1 min, and data was recorded. Figure 3 shows a schematic drawing of the calibration setup. Calibration range was from 0 to 5 m/s, which covers the expected range of air velocity values inside the container. The value 5 m/s was achieved by applying a flow of 650 SLM through MFC.

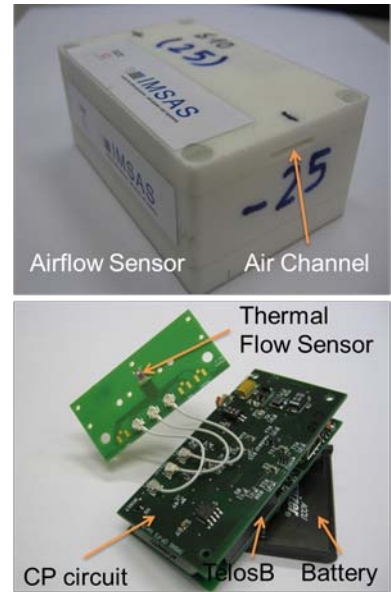


Figure 2: Airflow sensor with enclosure (top); four layers inside the enclosure (bottom).

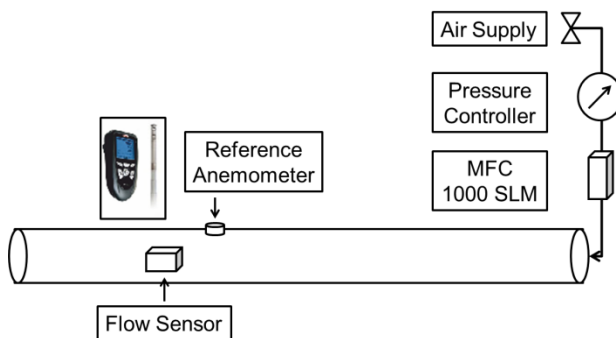


Figure 3: Airflow sensor calibration testbed. Both the reference and the flow sensor are shown here.

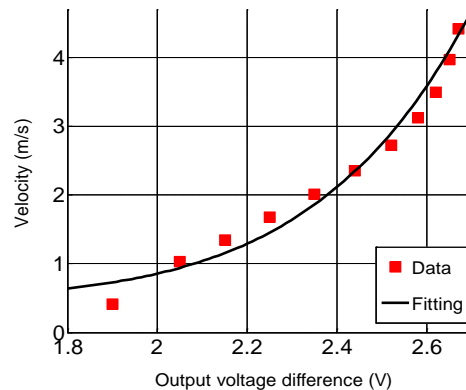


Figure 4: Example calibration curve: Airflow velocity of the reference anemometer (m/s) vs. Voltage output of the sensor.

The calibration procedure is repeated two times for each sensor, one for the positive velocities and the other for the negative ones. The calibration curves were found by means of a MATLAB fitting program. These curves follow the mathematical expression $v = a + b \cdot \Delta U^c$, where v is air velocity given in m/s; ΔU is the sensor output voltage difference given in Volt; a , b , and c are constants found by curve fitting for each sensor and for both directions.

By this way, each sensor has its own calibration curve—programmed into the FSU (see Section 3) as it is too energy exhaustive for the node to perform exponent-based arithmetic—which allows obtaining exact velocity values and consequently avoiding severe errors resulting from applying one calibration curve for all sensors. Figure 4 shows an example of a sensor calibration curve pertaining to one direction of air flow of one sensor. The R-squared value of the calibration equation used above is 0.97 in this example. It is higher than 0.9 for all fitted calibration curves, i.e. a good agreement is achieved between the experimental results and the fitted curves.

3 Field Tests

Airflow measurement field trials were carried out in the Intelligent Container. The container is equipped with a basestation that is connected to a FSU (Freight Supervision Unit). FSU is capable of relaying data from the basestation to a remote webserver. Fifteen wireless airflow sensors were placed in distributed locations in container with banana pallets and networked using the BananaHop protocol [7].

In all, eight different tests were conducted under two different banana loading schemes – four tests under the conventional loading scheme and four under the chimney-based loading scheme (i.e. pallets arranged in such a way that a top-to-bottom opening is formed in the middle of four surrounding pallets). Results presented in this paper pertain only to the conventional loading scheme. It is depicted in Figure 5(left): figure shows numbered banana pallets P1, P2...P11; the refrigeration unit is in the Reefer Side; the orientation of the banana pallets is denoted by P9 and P11; and, different levels of a pallet are denoted by Tier 1, Tier 2...Tier 8 (shortened as T1, T2...T8). The R1,2,3 depicted in Figure 5(right) represents the virtual lines on which the sensors were placed, both bottom and top of pallets.

A container can contain up to twenty banana pallets. But, both loading schemes used much less due to various logistical issues. Eleven banana pallets were used in the conventional loading scheme and twelve under the other. A removable but air tight partition was raised just after P9 and P11 (Figure 5), thereby creating an almost sealed and scaled-down banana container.

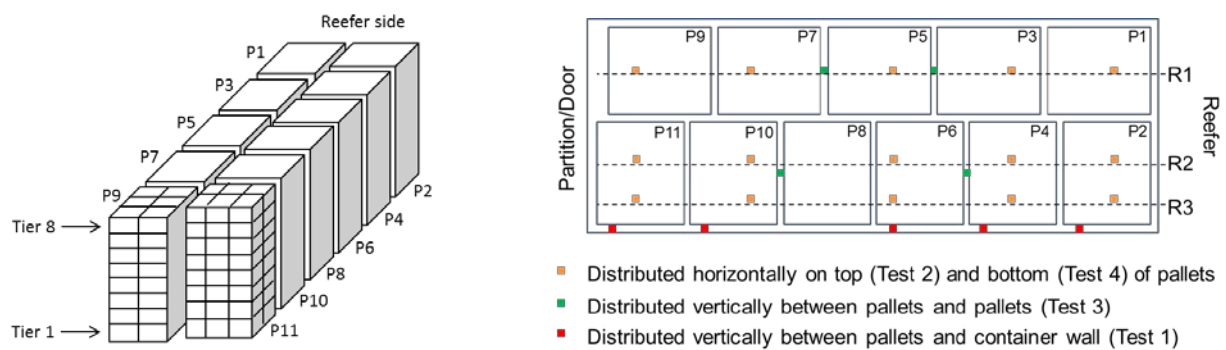


Figure 5: 3D perspective of the 11 pallets loaded in to the container (left); Birds eye view cross-section of a container showing the four types of sensor distributions under the conventional banana loading scheme (right).

The airflow sensors were placed mainly in four different gaps: between pallets and container walls (Test 1), above the pallets (Test 2), between adjoining pallets (Test 3), and below the pallets (Test 4). The sensor height from container bottom varies from test to test. However, for tests with vertical sensors placements, mainly Tier 1, 4 and 8 (T1, T4 and T8) were used: in some rare cases Tier 6 (T6) was used in addition. Tier number refers to the height level of a banana pallet, where Tier 1 is the bottom layer and Tier 8 is the highest layer. Figure 5(right) shows all areas where the sensors were placed in the four tests.

4 Measurement Results and Analysis

A major and unpreventable problem faced in the above mentioned four tests was the uneven gaps. Therefore, the measurement results showed arbitrariness and unpredictability in some measurements. A counter measure—a test with even gaps—to act as a pilot is planned for later.

In order to simplify the test results, not all sensor measurements in all tests are given. First, Test 1 (Figure 6(left)), the air flow measurement in vertical gaps between pallets and the container wall, is discussed. Then, Test 3 (Figure 6(right)), the vertical air flow spread in-between pallets is discussed. Test 2 and Test 4 describes how the airflow is distributed above and below the pallets. Figure 6 shows average airflow speeds of the sensors placed at different pallets and tiers as indicated on the x-axis;

P10/P8 means, for example, that the sensors were placed in the gap between these two pallets. Sensor data is organized as clusters: a cluster is defined as the sensors placed on one pallet. Missing columns in some clusters indicate that there were no sensors placed in those tiers. Air flow speeds indicated on all of the figures below are the speeds averaged over the duration of each test of each sensor. Duration of each test is taken as approximately four minutes after the reefer-start to reefer-stop of each test. Generally the air flow stabilizes after about four minutes of reefer-start.

In Test 1, considering T8 data, it is clearly seen that the airflow speed gradually increases towards the partition door side. The vertical air movement upwards is low near P1 due to high airflow speed at the outlet of the reefer unit, which is around 8-9 m/s. T1 data is evidently arbitrary, which is due to heavy turbulence by the ducts below the pallets and highly variable gaps between the pallet bottom and the container wall. Creation of variable gaps is unavoidable when loading the container.

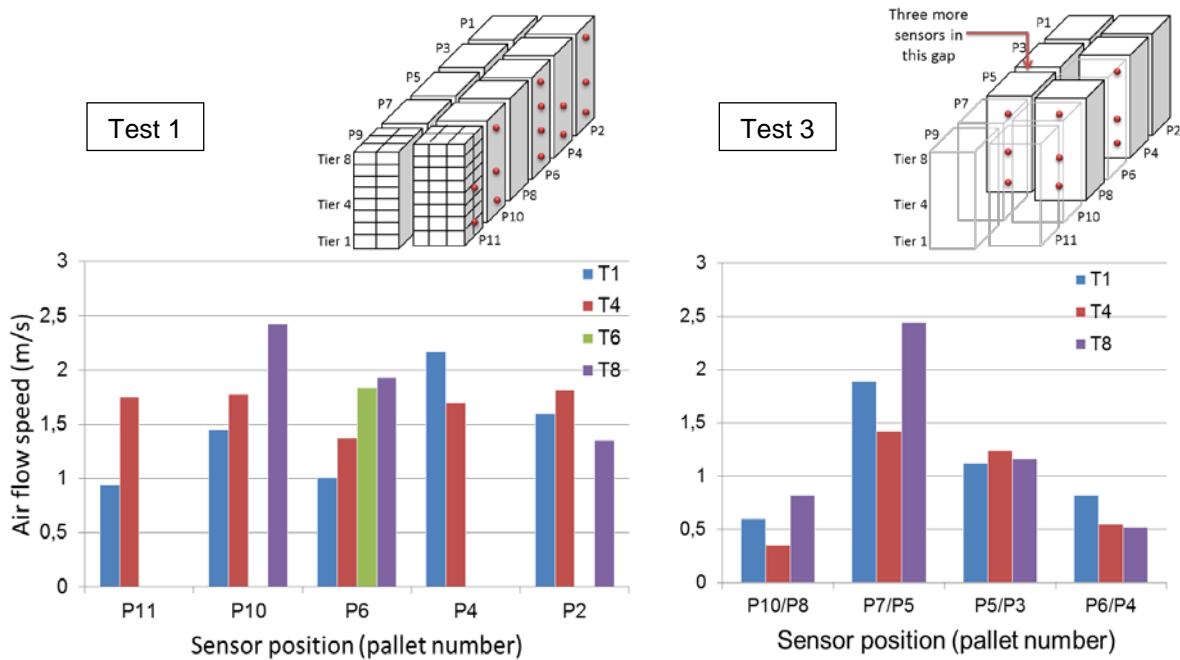


Figure 6: Average airflow speeds in Test 1 (left) and Test 3 (right). Vertical air movement upwards.

In Test 2, the sensors were mounted right on top of the pallets; the measured air flow speed was effectively 2.5 cm above the pallets. Therefore, as expected, the average speed measured for all sensors were low and below 0.72 m/s. In another test, two sensors were placed midway between the pallet top and container ceiling (30 cm above the pallets) to assess the airflow speed in that region, in locations above P3 and P7. Quite uncharacteristically they recorded 0.33 and 0.49 m/s, suggesting the air flow speeds just above the pallets were marginally higher than that of the speeds much above it.

In Test 3 (Figure 6(right)), very tight fit was observed in the gaps of P10/P8 and P6/P4 during the test. That is reflected well on the figure with very low air flow speeds. The other two gaps indicate relatively high, unimpeded air flow.

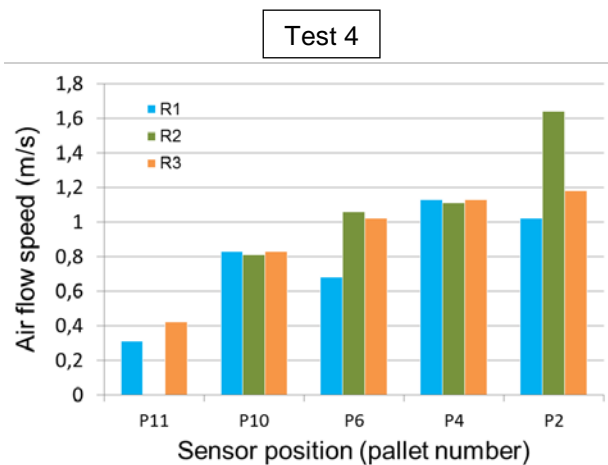


Figure 7: Test 4 – Air flow distribution at the bottom of the pallets (horizontal air movement). R1 R2, R3 is in accordance with Figure 5.

Test 4 results in Figure 7 clearly demonstrated the expected outcome. Air flow speeds near the reefer side was higher and it progressively reduced towards the door side.

5 Conclusions and Outlook

The undesired hotspots are a problem in perishable food transportation industry. A major reason for that is the lack of ventilation in certain areas of a refrigerated container. The historical records show no evidence of any data and analysis obtained in field trials on how the air flows in a container and how its lack of it adversely affects the temperature of produce. To facilitate distributed measurement of airflow within a container, a wireless sensor was produced using thermal flow sensors. The wireless sensors were also networked using the BananaHop protocol that overcame the challenge of heavy signal attenuation faced by any RF communication in high water content foods. Four tests were carried out using fifteen airflow sensors under the conventional banana loading scheme. Airflow speed in four different types of gaps was measured as a first step in analysis of the airflow patterns inside a refrigerated container. Some measurement results are inconclusive, mainly due to varying gap sizes that are inconsistent over each loading and unloading cycle. But, the airflow sensor proved to work very well in the container without failure. Also, the measurement results showed enough promise to conduct future tests.

Few steps are planned for the next field test: reducing the thickness of the air flow sensor, comparison of measurement results with a pilot test using consistent gaps as reference, comparison of different banana loading schemes, and relationship between temperature change of bananas and air flow.

References

- [1] Verdouw, C. N.; Sundmaeker, H.; Meyer, F.; Wolfert, J.; Verhoosel, J.: Smart Agri-Food Logistics: Requirements for the Future Internet. In: 3rd International Conference on Dynamics in Logistics (LDIC), Bremen, Germany, 2012, pp. 247-258. Doi: 10.1007/978-3-642-35966-8
- [2] Gustavsson, J.; Cederberg, C.; Senesson, Ulf.; van Otterdijk, R.; Meybeck, A.: Global Food Losses and Food Waste – Extent Causes and Prevention. SAVE FOOD! International Congress, Interpack2011, Düsseldorf, Germany. Food and Agriculture Organization of the United Nations, Rome 2011, Italy. pp. 4-8. Url: <http://www.fao.org/docrep/014/mb060e/mb060e00.htm>
- [3] The Intelligent Container. The intelligent container: Linked intelligent objects in logistics. Url: <http://www.intelligentcontainer.com/>, Accessed: 24.04.2013.
- [4] R. Buchner; M. Maiwald; C. Sosna; T. Schary; W. Benecke; W. Lang: Miniaturized thermal flow sensors for rough environments. In: 1⁹th IEEE International Conference on MEMS. Istanbul, 2006, pp. 582-585. Doi: 10.1109/MEMSYS.2006.1627866
- [5] S. Issa; C. Lloyd; W. Lang: Calibration and Uncertainty Estimation of Thermal Flow Micro-Sensor for Airflow Measurements, IGS Research Journal 2012/13, Vol. 3, pp. 23-26, 2013. [In-press]
- [6] Jedermann, R.; Moehrke, A.; Lang, W.: Supervision of banana transport by the intelligent container. In: Kreyenschmidt, J. (ed.): Coolchain-Management 4th International Workshop. University Bonn, Bonn, 2010, pp. 75-84.
- [7] Jedermann, R.; Becker, M.; Görg, C.; Lang, W.: Testing network protocols and signal attenuation in packed food transports. In: International Journal of Sensor Networks (IJSNet), Vol. 9 (2011) Nos. 3/4, pp. 170-181. Doi: 10.1504/IJSNET.2011.040238
- [8] Ashauer, M.; Glosch, H.; Hedrich, F.; Hey, N.; Sandmeier, H.; Lang, W.: Thermal flow sensor for liquids and gases. In: IEEE Conference on Micro Electro Mechanical Systems (MEMS) 1998, Heidelberg, Jan. 1998, proceedings 615-620. Doi: 10.1109/MEMSYS.1998.659781

Acknowledgments

The research project “The Intelligent Container” is supported by the Federal Ministry of Education and Research, Germany, under the reference number 01IA10001. We thank for the support by International Graduate School for Dynamics in Logistics (IGS) at the University of Bremen, and we are grateful for Dole Fresh Fruit Europe for the provision of test facilities.